

## Phase Separated BEC for High-Sensitivity Force Measurement

S. G. Bhongale<sup>1</sup> and Eddy Timmermans<sup>2</sup>

<sup>1</sup>*Department of Physics and Astronomy, MS 61, Rice University, Houston, Texas 77005, USA*

<sup>2</sup>*Center for Nonlinear Studies, LANL, Los Alamos, New Mexico 87545, USA*

(Received 22 November 2007; revised manuscript received 17 December 2007; published 5 May 2008)

A trapped, phase separated, two component Bose-Einstein condensate (BEC) can be configured to give a single BEC bubble that floats freely in the surrounding BEC. We point out that this system gives a unique template to carry out mesoscopic quantum studies and to detect weak forces. We demonstrate the detection capabilities by proposing and studying a “quantum level” for fundamental quantum fluctuation studies and for mapping the potential energy landscape near a surface with exquisite accuracy.

DOI: [10.1103/PhysRevLett.100.185301](https://doi.org/10.1103/PhysRevLett.100.185301)

PACS numbers: 67.60.-g, 03.75.Mn, 06.20.-f

The mesoscopic quantum coherent matter systems, such as dilute gas Bose-Einstein condensates (BEC's) and fermion superfluids, created in cold-atom traps are unusually sensitive and clean many-body systems that can be isolated nearly completely from the influence of environment, and possess unusual control knobs such as the ability to vary the interparticle interaction at will [1]. This has led to several suggestions for BEC probes that would measure, for example, Casimir forces [2], magnetic fields [3], or the earth's rotation [4]. In this Letter, we discuss the prospect of creating a mesoscopic sized BEC object (a BEC “bubble”) that is free or nearly free—the effective potential energy experienced by the bubble's center-of-mass position is nearly constant in space. Therefore, the bubble's center-of-mass position becomes an ultrasensitive measure of any weak external force on the bubble. At the same time, if the boundary region of the bubble is “sharp,” then its edge maps out potential energy contours with exquisite accuracy. The freely floating bubble also provides an intriguing template for probing mesoscopic quantum behavior. By crafting shallow external potentials superimposed upon the flat effective bubble potential, experimentalists could demonstrate many-body quantum interference, observe quantum Brownian motion, and study many-body quantum tunneling.

The actual bubble we propose to use is a trapped phase separated BEC of “B” atoms floating within a simultaneously trapped, larger BEC of “A” atoms [5] as shown in the schematic of Fig. 1. The extent of the phase separated BEC-B bubble is confined by the BEC-A sea in which it floats. By carefully choosing the trapping potentials and interaction strengths, the trapping, buoyancy, and surface tension forces on the bubble can cancel, resulting in a freely floating mesoscopic BEC object near the middle of the trap. An additional increase of the interspecies interaction strength decreases the size of the interface boundary region between the BEC's, sharpening the “edge” of the bubble. Now the bubble's position is extraordinarily sensitive to the magnitude of a small perturbing external force.

Thus, the position of the bubble becomes a measure of the magnitude of this force. Moreover, experimental methods based on imaging the shadow of the bubble as depicted in Fig. 1 can accurately measure the bubble displacement. Such techniques have proved to yield exquisitely precise position measurements elsewhere [6].

Conceptually, the proposed weak force detector resembles a “level”—a device that determines the horizontal direction by detecting the cancellation of the gravitational force component in the direction in which a bubble in a fluid-filled tube can move. At the point of cancellation, the bubble remains stationary in the middle of the tube. If the effective potential of the phase separated BEC bubble is exactly flat, then the actual ground state of the system is a superposition of states in which the bubble is located in different positions. If the bubble behaves as a macroscopic object, then once its position is measured, it remains

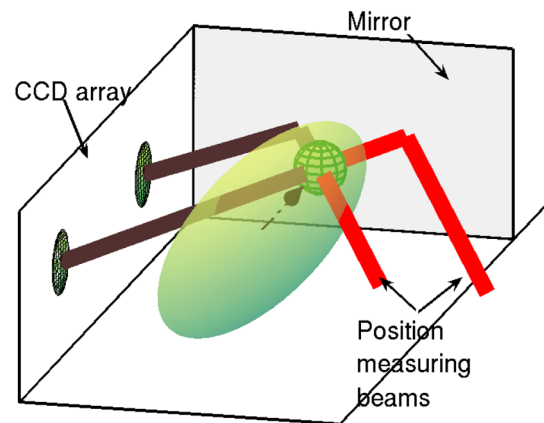


FIG. 1 (color online). Schematic of the proposed BEC level device. The bubble of BEC-B (represented by a sphere) is confined within the BEC-A sea (shown by the ellipsoid). The arrow along the axis of the ellipsoid is the direction of the external force that causes the bubble to be displaced from the center of the ellipsoid. This displacement can be measured by a laser configuration as shown in the figure.

localized, “pinned” by interactions with the environment—an essential ingredient of the breaking of translational symmetry. If the environment interactions are sufficiently weak and in the presence of a shallow double well potential, the bubble can behave as a quantum object, tunneling between the wells (the bubble’s surface tension may prevent single particle tunneling) or interfering with itself if it can follow different paths to reach the same final position. Such experiments that reveal the quantum properties of the bubble can be carried out on a “chip” [7] (near a surface). The main source of decoherence would be the excitation of phonon modes in the surrounding BEC sea.

For the discussion in this Letter, we will not require the extreme level of control necessary for the observation of mesoscopic quantum behavior. Instead, we assume that external interactions are present (though small) and that the BEC bubble acts as a classical object. Even in that case, the bubbles can probe genuine quantum effects, for example, the position of two bubbles each trapped in one well of a double well potential would be modified from their equilibrium position if they experience a mutual attraction, induced by a Casimir-like force arising from quantum fluctuations of the surrounding BEC [8].

We illustrate the cancellation of bubble forces in the case of a “small bubble of vanishing surface tension”—the simplest limit. In that case, the size of the bubble is sufficiently large to neglect the surface energy, but remains small compared to the length scale on which the trapping potentials  $V_A(\mathbf{r})$  and  $V_B(\mathbf{r})$  experienced by the  $A$  and  $B$  atoms, respectively, vary. Hence, we can replace  $V_B(\mathbf{r}) \approx V_B(\mathbf{R})$  where  $\mathbf{R}$  denotes the bubble’s center-of-mass position. We also assume that the BEC gas is dilute and that we can describe the interparticle interactions by the customary contact potentials:  $v_{A(B)}(\mathbf{r} - \mathbf{r}') = \lambda_{A(B)}\delta(\mathbf{r} - \mathbf{r}')$  for the mutual interactions of like bosons  $A$  (or  $B$ ) and  $v_{AB}(\mathbf{r} - \mathbf{x}) = \lambda\delta(\mathbf{r} - \mathbf{x})$  for the mutual interactions of unlike bosons. In a three-dimensional BEC gas, the contact interactions lead to local pressures within the single condensate regions of average density  $\rho_{A(B)}(\mathbf{r})$  equal to  $[\lambda_{A(B)}/2]\rho_{A(B)}^2(\mathbf{r})$ . If we neglect the surface tension of the bubble, then the condition of equilibrium requires the inside and outside bubble pressures to cancel, i.e.,  $P = \lambda_A[\bar{\rho}_A(\mathbf{R})]^2/2 = \lambda_B[\rho_B(\mathbf{R})]^2/2$ , where  $\bar{\rho}_A$  denotes the density of an all  $A$  BEC of the same chemical potential as the actual  $A$  BEC that surrounds the  $B$  bubble. Hence, the inside bubble density is equal to  $\rho_B(\mathbf{R}) = \sqrt{\lambda_A/\lambda_B}\bar{\rho}_A(\mathbf{R})$ . We write the ground state energy of the trapped BEC  $A$ , which has the  $B$  bubble of  $N_B$  particles immersed as the energy  $\bar{E}_A$  of all the  $A$  BEC that has the same chemical potential as the one with the bubble, and an integral over the  $B$  bubble volume  $\Omega_B$  centered on  $\mathbf{R}$ . Consistent with the assumption of slowly varying trapping potentials and the neglect of the bubble surface energy, we approximate the energy densities as  $V_{A(B)}(\mathbf{r})\rho_{A(B)}(\mathbf{r}) + [\lambda_{A(B)}/2]\rho_{A(B)}^2(\mathbf{r})$  and we obtain

$$\begin{aligned} E &= \bar{E}_A + \int_{\Omega_B} [V_B(\mathbf{r})\rho_B(\mathbf{r}) + \lambda_B\rho_B^2(\mathbf{r})/2] \\ &\quad - [V_A(\mathbf{r})\bar{\rho}_A(\mathbf{r}) + \lambda_A\bar{\rho}_A^2(\mathbf{r})/2]d\mathbf{r} \\ &\approx \bar{E}_A + N_B[V_B(\mathbf{R}) - \sqrt{\lambda_A/\lambda_B}V_B(\mathbf{R})], \end{aligned}$$

consistent with an effective potential energy per  $B$  particle equal to  $V_{\text{eff},B}(\mathbf{R}) = V_B(\mathbf{R}) - \sqrt{\lambda_B/\lambda_A}V_A(\mathbf{R})$ . Now, if the trapping potentials for  $A$  and  $B$  particles are simply proportional,  $V_A(\mathbf{r}) = \alpha V_B(\mathbf{r})$ , and we carefully tune the proportionality constant  $\alpha$  to  $\alpha \rightarrow \sqrt{\lambda_A/\lambda_B}$ , then the effective potential as seen by the bubble vanishes and it floats freely inside the BEC- $A$ .

This value,  $\alpha = \sqrt{\lambda_A/\lambda_B}$ , is also the proportionality constant at which the bubble’s position becomes highly sensitive to any small additional external force. We illustrate this for the case of harmonic trapping potentials,  $V_{B,\text{trap}}(\mathbf{r}) = (1/2)[K_x x^2 + K_y y^2 + K_z z^2]$ ,  $V_{A,\text{trap}}(\mathbf{r}) = \alpha V_{B,\text{trap}}(\mathbf{r})$ , to which a differential external force  $\mathbf{F} = \gamma\hat{z}$  (i.e., difference of force experienced by the  $A$  and  $B$  atoms) adds an approximately linear term to the  $B$  potential  $V_B(\mathbf{r}) = V_{B,\text{trap}}(\mathbf{r}) - \gamma z$ , so that

$$V_{\text{eff},B}(\mathbf{r}) = (1 - \alpha\sqrt{\lambda_B/\lambda_A})V_{B,\text{trap}} - \gamma z \quad (1)$$

$$\begin{aligned} &= [(1 - \alpha\sqrt{\lambda_B/\lambda_A})/2] \\ &\quad \times [K_x x^2 + K_y y^2 + K_z(z - \Delta)^2 - K_z\Delta^2], \quad (2) \end{aligned}$$

centered around a position that is displaced along the  $z$  axis from the former trap middle by a distance  $\Delta = \gamma[K_z(1 - \alpha\sqrt{\lambda_B/\lambda_A})]^{-1}$ . Hence, in equilibrium, the measurement  $\Delta$  provides a direct measurement of the magnitude of the force,  $|\mathbf{F}| = \gamma$ .

The accuracy with which the bubble’s position can be measured depends on the sharpness of its edge. In the edge region if we assume the respective BEC densities to vary as  $\rho_B(\epsilon) = \rho_B(\mathbf{R})(\delta - \epsilon)/\delta$  and  $\rho_A(\epsilon) = \rho_A(\mathbf{R})\epsilon/\delta$ , where  $0 \leq \epsilon \leq \delta$  is normal to the interface area  $\mathcal{A}$ , then the resulting kinetic energy contribution can be approximated by  $E_{\text{kin},\delta} = 4\mathcal{A}P[l_A^2 + l_B^2]/\delta$ , where  $l_{A(B)} = \hbar/\sqrt{4m_{A(B)}n_{A(B)}\lambda_{A(B)}}$  is the coherence length of BEC- $A(B)$ . We also find the surface interaction energy to be approximately equal to  $E_{\text{int},\delta} = \mathcal{A}P(\lambda - \sqrt{\lambda_A\lambda_B})\delta/3$ . Thus the equilibrium edge width obtained by minimizing this additional surface energy  $E_{\text{edge}} = E_{\text{kin},\delta} + E_{\text{int},\delta}$  is given by  $\bar{\delta} = \sqrt{12(l_A^2 + l_B^2)/(\lambda/\sqrt{\lambda_A\lambda_B} - 1)}$  [5]. Therefore the edge sharpness can be increased by increasing the interaction strength between unlike bosons by means of an interspecies scattering resonance [9]. This increases the importance of the surface energy, requiring either a description that includes surface tension explicitly or a numerical solution of the coupled Gross-Pitaevskii-like equations. Given the lack of space, we choose the latter

option and solve the numerical equations by evolving the Gross-Pitaevskii (GP) dynamics in imaginary time. Motivated by recent experiments with elongated BEC's [10] created by focusing a single laser beam, we consider a quasi-1D configuration with  $\omega_z$  and  $\omega_\perp$ , the trapping frequency in the axial and transverse directions, respectively, and  $\xi = \omega_z/\omega_\perp \ll 1$  for both species of bosons.

The wave functions,  $\phi_A$  and  $\phi_B$  of the two interacting condensates, evolve according to the coupled GP equations

$$i\phi_{A(B)} = \left[ \frac{-\nabla^2}{2} - \mu_{A(B)} + V_{A(B)}(\mathbf{r}) + \lambda_{A(B)} N_{A(B)} |\phi_{A(B)}|^2 \right] \phi_{A(B)} + \lambda N_{B(A)} |\phi_{B(A)}|^2 \phi_{A(B)},$$

where the mass of  $A$  and  $B$  atoms is assumed to be same,  $V_A(\mathbf{r}) = \alpha V_B(\mathbf{r}) = \alpha(x^2/2\xi^2 + y^2/2\xi^2 + z^2/2)$ , all the physical quantities are scaled in axial harmonic oscillator units, and the condensate wave functions  $\phi_{A(B)}$  are normalized to unity. We work in the phase separated regime by using  $\lambda/\sqrt{\lambda_A\lambda_B} = 1.1$ . The density profile obtained numerically is plotted in Fig. 2. In the same figure we also plot the value of the half axial length  $L$  obtained by neglecting surface tension and taking the Thomas-Fermi approximation. For treating the quasi-1D situation considered here, we use a modified local density ansatz given by  $\mu_{A(B)}(z) = \mu_{A(B)} - V_{A(B)}(z)$  and  $\mu_{A(B)}(z) = \sqrt{\alpha/\xi^2} \sqrt{1 + 4a_{A(B)}\rho_{A(B)}(z)}$  where  $a_{A(B)}$  is the two-body  $s$ -wave scattering length for atoms  $A$  ( $B$ ) [11], which

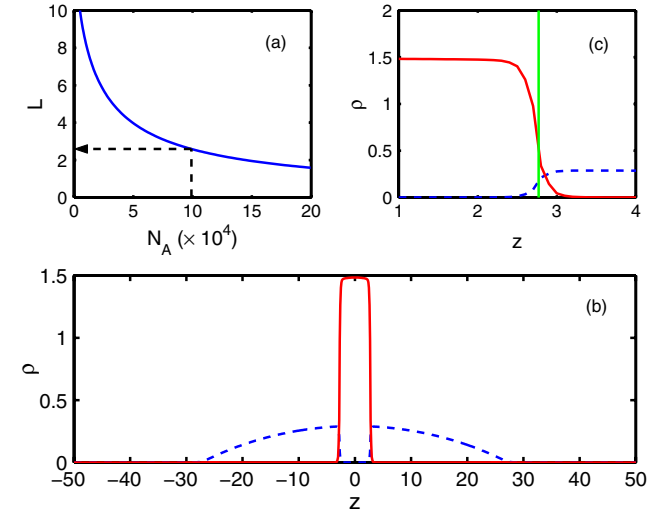


FIG. 2 (color online). Comparison of an analytical calculation that neglects the surface tension and the numerical GP solution. In (a) the half axial length  $L$  of the bubble is plotted as a function of  $N_A$  for  $N_B = 2 \times 10^4$ ,  $\alpha = 0.9$ ,  $\xi = 0.01$ ,  $\beta = 0.9$ , and  $a_A = 0.001$ , (b) the density profile obtained numerically for  $N_A = 10^5$  is shown, and (c) shows the magnified view of the interface region in (b). The green line indicates the boundary between BEC- $A$  and  $B$  obtained in (a).

determines the interaction strength by the relation  $\lambda_{A(B)} = 4\pi\hbar^2 a_{A(B)}/m$ . Figure 2(c) shows excellent agreement between  $L$  and the numerically obtained location of the bubble edge.

We demonstrate the working of the BEC level by considering an external force in the axial direction  $\mathbf{F} = \gamma\hat{z} = \bar{\gamma}(\hbar\omega_z/\ell_z)\hat{z}$ , where  $\ell_z$  is the axial trap length. As argued before, we tune the interatomic interactions such that  $\alpha\sqrt{\lambda_B/\lambda_A} \rightarrow 1^-$  and  $\lambda > \sqrt{\lambda_A\lambda_B}$ . The corresponding ground state density profile obtained numerically is shown in Fig. 3. Here we see that the BEC- $B$  bubble is displaced from the center of the trap by a distance  $\Delta \approx \bar{\gamma}/(1 - \alpha\sqrt{\lambda_B/\lambda_A})$ . The boson-boson interaction strength as well as the trapping frequencies can be precisely tuned in current cold-atom experimental setups resulting in a large displacement of the bubble and thus allowing for the precise measurement of  $|\mathbf{F}| = \bar{\gamma}$ . To estimate the sensitivity, let us consider, for example, a  $^{85}\text{Rb}$ - $^{87}\text{Rb}$  mixture where phase separation has recently been observed [12]. There the inter- and intraspecies scattering lengths are known accurately to about a percent [13], and thus we may assume  $\delta a/a \sim 10^{-2}$ . Now, for a small achievable trap frequency of 1 Hz (used in Ref. [10]), we immediately obtain the magnitude of the smallest measurable acceleration to be  $|\mathbf{F}/m| = \Delta\omega^2\delta a/2a = 5 \times 10^{-9} \text{ m/s}^2 \sim 5 \times 10^{-10}g$ , for a modest bubble displacement of 1  $\mu\text{m}$ , where  $g$  is Earth's gravitational acceleration. Thus, the proposed BEC level can measure exceedingly small accelerations over very small length scales. This estimated sensitivity value should be compared with other sensitive measurements based on, for example, atom interferometry and falling corner cube where  $\delta g/g \sim 10^{-9}$  [14].

While the above discussion was related to determining the force (gradient of the external potential), the proposed BEC level can also be used for mapping accurate potential

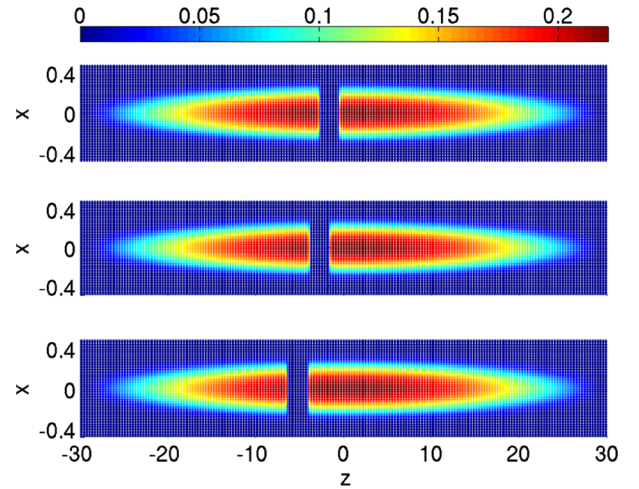


FIG. 3 (color online). Density of BEC- $A$  is shown as a surface plot for  $\bar{\gamma} = 0.1$ . The subplots top, middle, and bottom correspond to  $\alpha\sqrt{\lambda_B/\lambda_A} = 0.90, 0.93, \text{ and } 0.95$ , respectively. The BEC- $B$  bubble is located within BEC- $A$  where  $\rho_A(\mathbf{r}) = 0$ .



energy contours. In fact, such a measurement can be achieved using a single BEC as demonstrated in [10]. This experiment related the observed BEC-density profile to the variation of the external potential. The experimental accuracy of the potential was a few Hz with a spatial resolution of a few microns. One limitation of the potential measurement is set by the magnitude of the chemical potential. One cannot arbitrarily decrease the chemical potential or the density of the BEC will drop below what is necessary for imaging the atoms or, if the interparticle interaction is lowered, the coherence length of the BEC will increase to limit the spatial resolution. In contrast, the phase separated BEC configuration discussed in this Letter not only ensures large density inside the bubble allowing good imaging, but an edge width that can be reduced below typical BEC-coherence lengths allowing increased spatial resolution. We demonstrate this principle by considering an axially varying potential  $V_{\text{trap}}(z)$  as shown in the top-most subplot of Fig. 4. In the same figure, the remaining subplots show the density profile of the BEC-B as a function of the total number of A atoms,  $N_A$ . Here we see that as  $N_A$  is increased, the equilibrium size of the BEC-B bubble decreases. This continues till a point is reached when the BEC-B bubble is small enough and is localized in the valleys of the potential landscape. Moreover, as mentioned earlier, the edge sharpness can be improved by modifying the interspecies interaction strength  $\lambda$ . Thus, we see that the proposed BEC level device can map potential energy contours arising from, for example, surface magnetic fields with exquisite precision.

In conclusion, we have proposed a high-sensitivity device for measuring small forces (gradient of potential) by using a phase separated two component BEC configuration. The working of this device is analogous to that of a

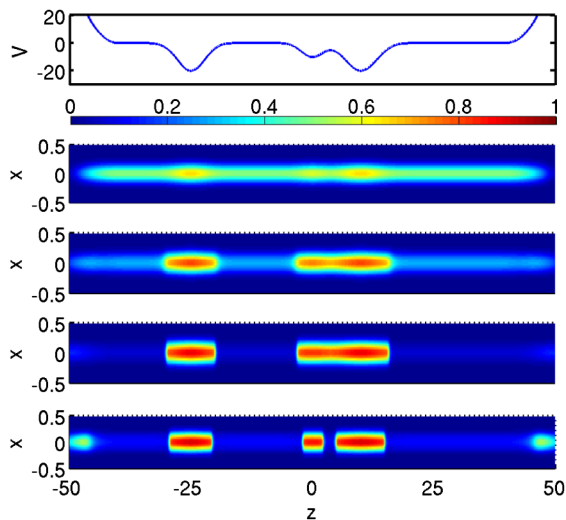


FIG. 4 (color online). Density profile of the quasi-1D BEC-B for different values of  $N_A$ . The topmost figure shows the trapping potential while the remaining four plots (from top to bottom) correspond to  $N_A = 0, 1000, 1500,$  and  $2000$ .

level, so that we named it a “BEC level.” This device can also map out potential energy contours with exquisite accuracy. This device could, for instance, map potential energy variations experienced by atoms near the surface of a metal caused by fluctuations of the surface fields. The BEC level provides several knobs that can be tuned, allowing for measurements to be carried out at multiple levels of accuracy.

While we have only exploited the bubble as a classical object, its possible range of explorations include mesoscopic quantum behavior such as many-body tunneling, quantum interference, and quantum Brownian motion. Thus, the idea of creating a mesoscopic object consisting of a dilute gas BEC not only gives rise to a new type of quantum measurement method, but also opens a whole new framework for cold-atom research within which numerous many-body quantum phenomena can be investigated via exploiting the proposed BEC level as a template.

S. B. acknowledges financial support from the W.M. Keck Program in Quantum Materials at Rice University. E. T. acknowledges support from the laboratory directed research and development (LDRD) program.

- 
- [1] C. Chin *et al.*, *Science* **305**, 1128 (2004); C. A. Regal, M. Greiner, and D. S. Jin, *Phys. Rev. Lett.* **92**, 040403 (2004); T. Bourdel *et al.*, *Phys. Rev. Lett.* **93**, 050401 (2004); K. M. O’ Hara *et al.*, *Science* **298**, 2179 (2002).
  - [2] J. M. Obrecht *et al.*, *Phys. Rev. Lett.* **98**, 063201 (2007).
  - [3] M. Vengalattore *et al.*, *Phys. Rev. Lett.* **98**, 200801 (2007).
  - [4] S. Stringari, *Phys. Rev. Lett.* **86**, 4725 (2001).
  - [5] Eddy Timmermans, arXiv:cond-mat/9709301; Eddy Timmermans, *Phys. Rev. Lett.* **81**, 5718 (1998); J. Stenger *et al.*, *Nature (London)* **396**, 345 (1998); D. S. Hall *et al.*, *Phys. Rev. Lett.* **81**, 1539 (1998); Also occurs in Fermi gases: G. B. Partridge *et al.*, *Science* **311**, 503 (2006).
  - [6] S. Schneider *et al.*, *Phys. Rev. A* **67**, 023612 (2003); D. M. Harber, J. M. Obrecht, J. M. McGuirk, and E. A. Cornell, *Phys. Rev. A* **72**, 033610 (2005).
  - [7] S. Aubin *et al.*, *Nature Phys.* **2**, 384 (2006); Ying-Ju Wang *et al.*, *Phys. Rev. Lett.* **94**, 090405 (2005); Y. Shin *et al.*, *Phys. Rev. A* **72**, 021604 (2005).
  - [8] D. C. Roberts and Y. Pomeau, *Phys. Rev. Lett.* **95**, 145303 (2005).
  - [9] M. Zaccanti *et al.*, *Phys. Rev. A* **74**, 041605 (2006), and references therein.
  - [10] P. Krüger *et al.*, *J. Phys.: Conf. Ser.* **19**, 56 (2005).
  - [11] F. Gerbier, *Europhys. Lett.* **66**, 771 (2004).
  - [12] S. B. Papp, J. M. Pino, and C. E. Wieman, arXiv:0802.2591.
  - [13] J. P. Burke Jr. and J. L. Bohn, *Phys. Rev. A* **59**, 1303 (1999); E. G. M. van Kempen, S. J. J. M. F. Kokkelmans, D. J. Heinzen, and B. J. Verhaar, *Phys. Rev. Lett.* **88**, 093201 (2002).
  - [14] A. Peters, K. Y. Chung, and S. Chu, *Metrologia* **38**, 25 (2001).